Experimental and Numerical Investigation of Dynamic Instability in Head Disk Interface at Proximity

Rohit P. Ambekar, Vineet Gupta and David B. Bogy

Computer Mechanics Laboratory
5150 Etcheverry Hall
Department of Mechanical Engineering
University of California
Berkeley, CA. 94720

Abstract

As the flying height decreases to achieve greater areal density in hard disk drives, different proximity forces act on the air bearing slider, which results in fly height modulation and instability. Identifying and characterizing these forces has become important for achieving a stable fly height at proximity. One way to study these forces is by examining the fly height hysteresis, which is a result of many constituent phenomena.

The difference in the touchdown and takeoff rpm (hysteresis) was monitored for different slider designs, varying the humidity and lubricant thickness of the disks, and the sliders were monitored for lubricant pickup while the disks were examined for lubricant depletion and modulation. Correlation was established between the observed hysteresis and different possible constituent phenomena. One such phenomenon was identified as the Intermolecular Force from the correlation between the lubricant thickness and the touchdown velocity. Simulations using 3D dynamic simulation software explain the experimental trends.

1. Introduction

In order to increase the recording density of magnetic hard disk drives (HDD), it is necessary to reduce the head-to-disk spacing. The head-to-disk spacing in the latest HDD has been decreased down to 10 nm. To achieve a magnetic recording areal density of 1 Tbit/in^2 it is expected that the physical spacing between the mean disk surface and transducer or flying-height (FH) will have to be 3.5 nm [1] or less. However, one of the major roadblocks in achieving this goal is the dynamic instability of the HDI.

It has been experimentally observed that a dynamic instability occurs in the fly height in the sub 5nm flying regime. The observed phenomena have been modeled primarily as resulting from intermolecular forces [2] and meniscus forces [9-12, 18]. The objective of this research is to investigate this fly height instability in detail and determine the contributing factors.

Extensive research has been conducted in the past few years on the dynamic instability of airbearing sliders in HDD at proximity to understand the various phenomena occurring and to achieve a stable flying height in the sub 5nm regime. Different analytical models have been developed. One goal of the many models has been to predict the experimentally observed fly height hysteresis.

Hysteresis is a common phenomenon in a variety of materials and processes. It is prominent in Atomic Force Microscopy (AFM) [13], and analytical models explain this hysteresis by the presence of meniscus forces, where the liquid (absorbed water on the surface of the material) forms a meniscus bridge when the AFM tip comes into contact with the sample. This meniscus exerts an attractive force on the tip and it ruptures at a much larger spacing when the tip retracts, thus demonstrating hysteresis [13]. In HDI, the presence of a lubricant / adsorbed water layer creates a similar situation. Hence, bridge models have been proposed using the meniscus force to explain the touchdown-takeoff hysteresis observed in HDD [18].

However, the lubricant layer in the HDI is very thin (~ monolayer), strongly bonded to the protective carbon overcoat and has only a small fraction of free mobile lubricant to form the meniscus. Also, the average time of contact during the "bouncing" is of the order of 10^{-9} seconds, and this is far from the equilibrium state predicted by the kinetic meniscus formation model [9].

A variety of proximity phenomena have been explained by intermolecular adhesion force models. These forces are primarily a result of electrostatic attraction between two atoms/ molecules due to their unbalanced electron clouds, leading to a dipole formation [6]. These forces can be very large when two surfaces are in close proximity (~ atomic distances).

The effect of intermolecular forces on HDI dynamic performance was first considered by Wu and Bogy [2]. Thornton and Bogy [3] demonstrated the observed experimental instability at proximity and hysteresis by a 1-DOF model using intermolecular forces (Lennard-Jones potential). Thus, hysteresis has been analytically demonstrated as a result of meniscus forces as well as intermolecular force. Hence, experimental investigation is needed to determine the various factors/ interactions that cause this hysteresis and the dynamic instability. This was achieved in the research presented here by conducting spindown-dwell-spinup (SDS) tests under varying conditions of humidity and lubricant thickness. The touchdown-takeoff rpm (hysteresis) was monitored, and correlation was established between the observed phenomena and the variation in the experimental parameters.

2. Rationale:

Different forces act on the slider in proximity that influence the dynamic stability of the head-disk interface. Some of these forces may arise from contact of the slider and the disk, such as the development of menisci, while some may be non-contact short range forces, such as the external excitation of the low flying slider by lubricant modulation, or the presence of intermolecular forces.

The phenomenon of hysteresis has two components – touchdown and takeoff. Care is taken so that the slider is never in contact before the touchdown occurs, so the variation in the touchdown can be attributed to the variation in non-contact forces. The two major non-contact forces are considered to be the intermolecular forces and the external excitation caused by the lubricant modulation [19]. If further, the touchdown variation is studied keeping the lubricant modulation variation to the minimum (achieved by using a disk with high bonded lubricant ratio, and dwelling on the experimental track on the disk for not more that 10 seconds), the other non-contact force (intermolecular

force) can be investigated for its existence and its effect can be studied on the dynamic instability.

Using this rationale, the presence of intermolecular forces can be determined by monitoring the touchdown rpm while the meniscus forces can be determined by takeoff rpm. The variation in the touchdown and takeoff rpm can be used to study the effects of intermolecular and meniscus forces, respectively.

In this report we describe an experiment to identify the factors contributing to the dynamic instability and present the experimental results. Experimental evidence of the presence of intermolecular forces is established.

The experiment was carried out in a controlled environmental chamber (Figure 1) with the CETR tester equipped with a wide bandwidth acoustic emission (AE) sensor. The effect of hysteresis was studied for different values of humidity, slider design and lubricant thickness, and inferences were made from the observations.

It is concluded that the touchdown velocity is affected by the thickness of the lubricant on the disk. Further, the hysteresis is affected by other phenomena such as lubricant pickup by the flying slider. The change in the ambient humidity (0-60% RH) did not show any particular trend in the hysteresis observed.

Experimental Section

3. Experimental Setup:

Figure 1(a),(b) and 2(a),(b) show the various apparatus used to conduct the experiment. Figure 1 (a) shows an apparatus to achieve controlled environment. A low pressure of 5 mTorr is achievable. A CETR tester was modified, and set up inside the environmental chamber. First, a L/UL test was conducted with an 18nm FH slider using the velocity profile shown in Figure 4. Disks of various lubricant thicknesses were used for the experiments (described in Table 1). The touchdown-takeoff hysteresis process was monitored by an AE sensor. This is a very reliable method of detecting contact [5].

(i) Dependence on humidity:

In the presence of ambient humidity water is adsorbed onto the disk surface [14]. This, as well as the mobile lubricant layer may aid in the formation of a meniscus and thereby contribute to the meniscus forces. The spindown-spinup tests were conducted for disks with a high ratio of bonded lubricant at zero humidity and at ambient humidity. The procedure of the tests is briefly described as follows:

The 18nm FH slider (Figure 3(a)) was loaded on to the rotating disk with the designed z-height. The slider was then unloaded onto a L/UL ramp, and the chamber was closed with the belljar. The disk rotation was stopped and the chamber was pumped down to a lower pressure depending upon the final humidity desired in the chamber. To achieve zero humidity in the environmental chamber, N_2 gas (ultra high pure-UHP) was pumped into the chamber. The final experimental conditions were ambient pressure and temperature and the desired humidity.

In the tests conducted later, low flying sliders (5nm and 7nm CML) of the CSS type were used. Since the pressure in the belljar could not be pumped down very low, a different CSS tester with its hood was modified into an environmental chamber (Figure 1(b)), in which N_2 gas could be pumped into the chamber through a pipe. The chamber was provided with a small aperture at the opposite end to force the excess gas out. The pumped gas mixed with the ambient gas in the chamber decreasing the humidity, and forcing the ambient gas out from the chamber. A humidity sensor kept inside the chamber measured the humidity.

In the tests conducted, the same slider was used on different tracks on a disk and without cleaning. After a test sequence, the slider was observed with a microscope to observe lubricant/debris pickup.

(ii) Dependence on lubricant thickness:

While keeping the humidity constant (ambient ~ 40%RH), we conducted the tests using INSIC CML sliders (7nm and 5nm) for various values of lubricant thickness. Each run was conducted on a different track, and with a clean slider. The slider and the disk were monitored after the tests using the microscope and the Candela OSA (Figure 2(a),(b)) respectively. The tests were conducted in the order of lubricant thicknesses of 1.2nm – 0.8nm – 2.0nm or 1.2nm – 2.0nm – 0.8nm.

First, the tests were conducted using the CETR and the actual AE signal amplitudes (filtered with a high order filter in MATLAB) were plotted against the velocity (Figures 5,6,7,8). The test was programmed with the software of the CETR. The disk starts rotating and attains a speed of 8000 rpm, at which time the slider is lowered onto the disk at 1.6" with the required z-height. The actuator then seeks to the required track (being used for the run), and the disk speed is lowered to a value such that a slight slider-disk contact is expected. (This value of rpm is set by performing sample runs on a particular slider-disk combination.) The disk dwells at the minimum rpm for 1 second, and then it is accelerated at the same rate at which it was decelerated (symmetric velocity profile). After reaching the final speed of 8000 rpm, the actuator seeks to the 1.6" track and is loaded off the disk, while the disk is dwelling at 8000 rpm. The disk is then decelerated to a halt. Both, the slider and the disk are then removed from the CETR tester. The slider is observed under the microscope for lubricant pickup and the disk is observed on the Candela OSA for lube depletion and modulation.

In order to verify that the AE signal corresponds to the slider-disk contact, similar tests were performed on a TTi tester having both AE and LDV measurement capabilities. The AE and LDV signals both showed spikes at the same instant indicating most likely contact (Figure 9).

The disks used in these tests were 95 mm ultra smooth disks (~0.2 nm RMS roughness), with aluminum substrate, magnetic layer, 3nm CHN overcoat and lubricant of varying thickness, with a bonded-mobile ratio of about 1:1. The disks were of the same make, and hence were expected to have same waviness.

(iii) Dependence on slider design

The dependence of the hysteresis on slider design was also studied along with the effect of lubricant thickness. The various sliders which were used in these tests are shown in Figure 3. They had fly heights of 18nm (pico), 7nm (pico) and 5nm (pico, with new suspension and old).

4. Results:

The results of the previously described experiments are presented in this section:

(i) Dependence on humidity:

The results of the SDS test conducted at zero humidity are shown in Figure 5. As can be seen there, a hysteresis occurs at zero humidity, for lubricant with a high bonded ratio and in absence of slider lubricant pickup. This is a case in which formation of a meniscus is very difficult, and it implies that meniscus forces, if they affect at all, cannot be the only contributing factor to the hysteresis observed.

The effect of humidity on the mobility of the lubricant and its bonding to the carbon overcoat has been studied previously [15, 16]. An increase in humidity may weaken the lubricant-carbon overcoat bonding because the adsorbed water may diffuse into the carbon surface and form bonds with the active sites on the carbon surface. This also reduces the diffusion energy barrier (due to intermolecular and lubricant-disk interactions) that the lubricant molecules have to overcome in order to move from one area to another, thereby increasing the lubricant mobility.

The effect of humidity also depends on the terminal group reactivity of the lubricant. The lubricant-overcoat bonding is stronger in the case of a more reactive terminal group [15].

However, from the tests conducted, it appears that hysteresis does not have a strong dependence on humidity (Figure 6). Figure 7 shows extreme hysteresis (solid curve). This was attributed to severe lubricant pickup by the slider as observed under the microscope. Thus, other factors such as lubricant pickup do seem to have some bearing on the hysteresis observed.

(ii) Dependence on lubricant thickness:

Experiments for studying the effect of lubricant thickness on the hysteresis were conducted. It was observed that the touchdown speeds were greater for low flying sliders. A plot of AE versus the disk velocity (rpm) for various lubricant thicknesses is shown in Figure 8. The experiments were conducted on the CETR tester at ambient humidity (40% RH). The Candela lubricant depletion profiles corresponding to each lubricant thickness are shown in Figures 10 and 11 for the 7nm and 5nm FH sliders, respectively. These

results are opposite to what has been obtained were opposite to that obtained by other authors [7]. Therefore, to verify the results, similar tests were conducted on a variety of other slider designs. The same trend was obtained for each ABS design. Figure 10 shows the touchdown variation for various slider designs for tests conducted at 0˚ skew at radius of 1.45".

This observed trend in the variation of the touchdown rpm is believed to be a result of a variation in non-contact forces, which are, in turn, a result of slider-lubricant interactions (causing lubricant modulation/depletion) and intermolecular forces. Lubricant modulation provides external excitation to the low flying slider which may cause a touchdown at higher rpm.

Lubricant modulation profiles before touchdown cannot be observed, as there is severe contact of the slider and the disk, which causes lubricant depletion. Lubricant depletion provides some estimate of the amount of mobile lubricant on the track before the touchdown occurs. It also relates to the severity of contact during the SDS test. Larger lubricant thickness with more mobile lubricant will have more lubricant modulation and depletion. Hence, the touchdown velocity is expected to be higher for thicker lubricants.

There was some difference in the lubricant depletion profiles. For example, in Figures 10 and 11, the 8Å, 12Å and 20Å disks had lubricant depletion of 5 Å, 3.3 Å and 20 Å respectively for the 5nm, and 2.5 Å, -3.3 Å and 5 Å respectively for the 7nm (negative sign indicates a lubricant buildup). The important observation to be made is that even though more modulation can be expected for higher lubricant thickness which should cause a higher touchdown velocity, the observed results should show a contrary trend. Hence, there must be present a strong attractive non-contact force which overcomes the effect of lubricant modulation and influences the observed trend. These evidences lead us to conclude the presence of a strong attractive intermolecular force at proximity.

(iii) Dependence on slider design

The touchdown velocity was observed to be dependent on the slider design. It was found to be higher for low flying sliders (Figure 10). The effect of intermolecular force is stronger for low flying sliders. Hence, the touchdown velocity will also be higher.

Furthermore, less lubricant depletion was observed. Also it does not vary much with the lubricant thickness variation. Hence, the variation in the touchdown rpm can be correlated with the fly height of a slider as a function of rpm.

After obtaining the experimental trends, simulations were done to see if the inclusion of intermolecular forces in the presence of different lubricant thicknesses yielded similar trends to those observed in experiments.

Simulation Section

5. Modeling of Intermolecular Forces:

Intermolecular forces are close range forces. They constitute of a (relatively) long range attractive force and a short range repulsive force and can be modeled by the Lennard-Jones Potential.

$$F(r) = -\frac{A}{r^6} + \frac{B}{r^{12}} \tag{1}$$

where, r = distance between the particles/ molecules /atoms

A, B = Hamaker constants (A ~ 10^{-19} J and B ~ 10^{-76}Jm^6)

F(r) = Intermolecular force (function of distance, *r*)

The intermolecular force model was incorporated into the CML Air software. In this software, the calculation of intermolecular forces between the slider and disk surfaces is done at every node in the mesh, and attractive and repulsive forces are calculated by summing the individual forces on the nodes to give value of the total intermolecular force. From equation (1), it is seen that the attractive component of the intermolecular force depends on the Hamaker constant A. This constant, is specific to material combinations.

Typically, the range of action of this force is ~10 nm. Hence, for low flying sliders, it is not only interaction between the topmost layers (lubricant on the disk and DLC on the slider) that counts, but other layers in both, disk and slider influence the interaction. Since both, the slider and the disk are layered, there is a multilayer interaction (Figure 13), and the method for calculating the Hamaker constant A is given by Lifshitz

theory [6]. According to this theory, the Hamaker constant for two materials, 1 and 2, interacting across a medium 3 is given by:

$$A_{132} = \frac{3}{4} k\bar{T} \left(\frac{\varepsilon_1 - \varepsilon_3}{\varepsilon_1 + \varepsilon_3}\right)\left(\frac{\varepsilon_2 - \varepsilon_3}{\varepsilon_2 + \varepsilon_3}\right) + \frac{3h\nu_e}{8\sqrt{2}} \frac{(n_1^2 - n_3^2)(n_2^2 - n_3^2)}{(n_1^2 + n_3^2)^{1/2}(n_2^2 + n_3^2)^{1/2}\{(n_1^2 + n_3^2)^{1/2} + (n_2^2 + n_3^2)^{1/2}\}} \tag{2}$$

where, ε_i = permittivity of material *i* ($C^2J^{-1}m^{-1}$),

n_i = refractive index of material *i*,

υ_e = 3 x10^{15} Hz (ionization frequency),

h = ($2\pi\hbar$) = Planck's constant, (6.626x10^{-34}Js),

k = 1.381x10^{-23} JK^{-1} (Boltzmann's constant), and

$\bar{T}$ ~ 300 K (Temperature at the interface)

The Hamaker constant, and thus the intermolecular forces depend on the refractive index and the permittivity of a material. Change in these properties, cause increase or decrease of intermolecular forces between the slider and the disk. However, since both, the slider and the disk have multiple layers, and further, they are thin enough (~2-20 nm) to contribute to the intermolecular forces, multilayer effects have to be considered. The multilayer model (Eqn. 11.37) derived in [6] is not applicable to the Head Disk Interface because the sign of the combining relations used in order to derive it has to be changed by the combination of materials [17]. The equation for multilayer model is derived for a 4 layer model by Matsuoka et. al. [17] as:

$$F(D_l) = -\frac{1}{6\pi}\left[\frac{A_{232'3}}{{D_l}^3} + \frac{A_{2'312}}{(D_l + T)^3} + \frac{A_{231'2'}}{(D_l + T')^3} + \frac{A_{121'2'}}{(D_l + T + T')^3}\right]\Delta x \Delta y \tag{3}$$

where,

$$A_{ijkl} = \frac{3h\nu_e}{8\sqrt{2}} \frac{(n_i^2 - n_j^2)(n_k^2 - n_l^2)}{(n_i^2 + n_j^2)^{1/2}(n_k^2 + n_l^2)^{1/2}\{(n_i^2 + n_j^2)^{1/2} + (n_k^2 + n_l^2)^{1/2}\}} \tag{4}$$

and,

D_l = Fly height of the slider (nm)

T = Thickness of disk lube (nm)

T' = Thickness of head DLC (nm)

and rest of the symbols have their meaning as explained above (after equation (2)). Note that the first term in equation (2) containing permittivity is not included in equation (4) as it is an order of magnitude smaller than the second term.

This equation was used to calculate the intermolecular force between the slider and the disk in the CML Air software. For the head disk interaction two layers on the disk (lube, DLC) and two layers on the slider (DLC, Al_2O_3-TiC), i.e. a total of 4 layers were considered to be interacting across air as the medium. Thus, the 4-layer model was used to obtain the results. The Hamaker constants were calculated using the permittivities and refractive indices of the various layers (Table 1). It was found that the Hamaker constant for DLC was greater than that of lubricant. Hence, the lesser the thickness of the lubricant, the more the influence of disk DLC on the head disk interface. Thus, an increase in the intermolecular force maybe expected when lubricant thickness is reduced.

Using the thicknesses given in Table 1, and varying the thickness of the lubricant, we completed simulations at a radius of 1.45" (36.8 mm) and 0˚ skew with the CML Air software.

The results are shown in Figure 14, 15 and 16. In Figure 14, it is seen that as the lubricant thickness increases, the magnitude of intermolecular force decreases. Also, as the fly height decreases, there is more of an increase in the intermolecular forces with decreasing lubricant thickness, i.e., the effect of change in lubricant thickness will have a larger effect on flyability of the slider for lower flying heights.

This can be explained on the basis of the values of the Hamaker constants calculated (Table 2). We note that $A_{232'3}$ and $A_{2'312}$ are dominant as compared to $A_{231'2'}$ and $A_{121'2'}$. $A_{232'3}$ corresponds to disk lube – head DLC interaction through air while $A_{2'312}$ corresponds to disk DLC – head DLC interaction with multilayer effect of air and disk lube included. When D_l and T are equal, we see that $(D_l+T)^3 = 8*D_l^3$. Thus, $A_{232'3}$ will be the dominant term whenever there is more lubricant. This is consistent with the physical explanation that the properties of the closest layers at the interface will be more

dominant. The thicker these layers become, the further away from the interface the back layers (1' and 1) are, and the lesser the influence they wield. However, this also indicates that as the lubricant layer gets thinner, the effect of disk DLC will be dominant, esp. because it has a higher Hamaker constant value associated with it. From Figure 14, it is seen that at FH=1.5 nm, IMF (lube=0 nm) = -0.66 gm and IMF (lube=2.0 nm) = -0.42 gm, an increase of 57% in the intermolecular forces. These forces are significant as they are comparable to the gram loads applied to the sliders (1.5 gm for pico).

For higher fly heights, when $D_l >> T$, $(D_l+T) \approx D_l$. Thus, the effect of $A_{232'3} < A_{2'312}$ is not as acute as when $D_l \approx T$ holds, and hence, there is only a small variation in the intermolecular forces due to change in the lubricant thickness for higher flying heights, as seen in Figure 14.

In Figure 15, the fly height diagrams obtained from the simulations are plotted. The upper curves correspond to stable flying heights, while the lower ones correspond to unstable flying heights [3]. During spindown, as the rpm reduces, the fly-height of the slider reduces along the upper (stable) curve. At the bifurcation point shown in the graph, there is a transition of the slider from a stable regime to a contact. The rpm at which this transition takes place is defined as the touchdown rpm for the simulation results and it has been plotted for two sliders corresponding to various lubricant thicknesses in Figure 16. It is seen that the experimental (Figure 10) and simulation (Figure 16) results exhibit similar trends: the touchdown velocity is higher for thinner lubricants and low flying sliders. This is primarily the result of the increase in the intermolecular forces due to reduction in the lubricant thickness.

6. Discussion:

The differences in the touchdown rpm relate to the variation in non-contact forces, which for the head disk interface have been primarily identified as the intermolecular forces and external excitation due to lubricant modulation or changes in the flying conditions due to lubricant depletion (lubricant non-uniformity). In the experiments conducted, care was taken to keep the variation of the lubricant modulation/depletion limited. Hence, the variation of the touchdown rpm (which was

counter to the trend meniscus forces would predict) was attributed to the presence of the other proximity non-contact forces, the intermolecular forces.

In an SDS test, as the disk rpm reduces, the slider flies lower. Hence, an increase in the attractive force due to a decrease in lubricant thickness may lead to early touchdown. Simulations using a multilayer model, varying the lubricant thickness, indicate that as the lubricant thickness decreases, there is more adhesion force due to intermolecular forces. This explains the experimentally observed phenomenon: The touchdown rpm is higher for thinner lubricants.

7. Conclusions:

Monitoring the touchdown and takeoff velocity while varying the parameters such as lubricant thickness and humidity can give information about various head disk interactions at proximity. The experimental trends obtained were correlated with the possible factors that could cause them, and the presence of intermolecular forces was concluded as a primary cause on the basis of the following observations:

(a) Hysteresis can be a result of many phenomena occurring at the head-disk interface. Hence, to make conclusions about the effects of a particular interaction, it is necessary to isolate each interaction on the basis of its nature (contact or non-contact) and its domain of operation.

(b) Hysteresis was observed at zero humidity for a lubricant with a high bonded ratio, leading to a conclusion that a meniscus force may not be the primary contributor to the observed hysteresis.

(c) Most importantly, the variation in the touchdown rpm is due to a non-contact force. Since lubricant non-uniformity is small, the variation must be due to a variation in the intermolecular forces.

(d) Simulations conducted with the inclusion of a multilayer model of intermolecular forces into CML Air software predicted results consistent with the observed experimental trends.

Acknowledgements:

This work was supported by the Computer Mechanics Laboratory at the University of California, Berkeley, USA and the Information Storage Industry Consortium (INSIC).

References:

[1] Wood, R., 2000, "The Feasibility of Magnetic Recording at 1 Terabit per Square Inch," IEEE Transactions on Magnetics, **36**, January, pp. 36-42.

[2] Wu, L., and Bogy, D. B., 2002, "Effect of the Intermolecular Forces on the Flying Attitude of Sub- 5 NM Flying Height Air Bearing Sliders in Hard Disk Drives," ASME J. of Tribology, **124**, July, pp. 562-567.

[3] Thornton, B.H., and Bogy, D.B., "Head-Disk Interface Dynamic Instability due to Intermolecular Forces," 2003, IEEE Transactions on Magnetics, **39** (5), September, pp.2420-2422.

[4] Zhang, B., and Nakajima, A., 2003, "Possibility of Surface Force Effect in Slider Air Bearings of 100 Gbit/in^2 Hard Disks," Tribology International, **36**, pp. 291-296.

[5] Jeong, T.G., 1991, "Slider-Disk Interactions during Dynamic Load-Unload in Magnetic Recording Disk Drives," Ph.D. Thesis, University of California at Berkeley.

[6] Israelachvili, J. N., 1992, *Intermolecular and surface forces,* 2nd edition, San Diego, Academic Press.

[7] Knigge, B., and Talke, F., 2001, "Nonlinear Dynamic Effects at the Head Disk Interface", IEEE Transactions on Magnetics, **37**, March, pp. 900-905.

[8] Gitis, N., and Volpe, L., "Nature of Static Friction Time Dependence," 1992, J. Phys. D: Appl. Phys., **25**, pp. 605-612.

[9] Bhushan, B., Kotwal, C.A., and Chilamakuri, S.K., 1998, "Kinetic Meniscus

Model for Prediction of Rest Stiction," ASME J. of Tribology, **120**, January, pp. 42-50.

[10] Kato, T., Watanabe, S., and Matsuoka, H., "Dynamic Characteristics of an In-Contact Headslider Considering Meniscus Force: Part 1—Formulation and Application to the Disk with Sinusoidal Undulation," 2000, ASME J. of Tribology, **122**, July, pp. 633-638.

[11] Kato, T., Watanabe, S., and Matsuoka, H., "Dynamic Characteristics of an In-Contact Headslider Considering Meniscus Force: Part 2 – Application to the Disk with Random Undulation and Design Conditions," 2001, ASME J. of Tribology, **123**, January, pp. 168-174.

[12] Kato, T., Watanabe, S., and Matsuoka, H., "Dynamic Characteristics of an In-Contact Headslider Considering Meniscus Force: Part 3 – Formulation and Application to the Disk with Sinusoidal Undulation," 2002, ASME J. of Tribology, **124**, October, pp. 801-810.

[13] Zitzler, L., Herminghaus, S., and Mugele, F., "Capillary Forces in Tapping Mode Atomic Force Microscopy," 2002, Physical Review B-Condensed Matter, **66**(15), October, pp.1554361-8.

[14] Shukla, N., Svedberg, E., van de Veerdonk, R.J.M., Ma, X., Gui, J. and Gellman, A.J., "Water Adsorption on Lubricated a-CH_x in Humid Environments," 2003, Tribology Letters, **15**(1), pp.9-14.

[15] Dai, Q., Vurens, G., Luna, M. and Salmeron, M., "Lubricant Distribution on Hard Disk Surfaces: Effect of Humidity and Terminal Group Reactivity," 1997, Langmuir, **13**, pp.4401-4406.

[16] Lei, R.Z., and Gellman, A.J., "Humidity Effects on PFPE Lubricant Bonding to a-CH_x Overcoats," 2000, Langmuir, **16**, pp. 6628-6635.

[17] Matsuoka, H., Ohkubo, S., and Fukui, S., "Dynamic Characteristics of flying Head Slider considering Van der Waals Forces (Analyses based on the Corrected Van der Waals Force Equation for Multilayers)," 2003, Proceedings of 2003 STLA/ASME Joint International Tribology Conference, Florida, October, pp. 51-57.

[18] Iida, K., and Ono, K., "Design Consideration of Contact/Near-Contact Sliders

based on a Rough Surface Contact Model," ASME J. of Tribology, 2003, **125**(3), July, pp. 562-70.

[19] Watanabe, T., and Bogy, D.B., "A Study of the Lubricant Displacement Under a Flying Head Slider Caused by Slider-Disk Interaction," 2003, IEEE Transactions on Magnetics, **39**(5), September, pp.2477-9.

Layer	Permittivity (ε_i)	Refractive Index (n)	Layer Thickness (nm)
Head Al_2O_3-TiC	11.54	1.75	∞
Head DLC	2.418	1.9	2.5
Air	1.0	1.0	Fly height
Disk Lubricant	2.2	1.3	0 - 2 <varied>
Disk DLC	2.418	1.9	∞

Table 1: Properties of different layers at the Head Disk Interface (as used for simulations) [4, 18].

Hamaker Constants ($x10^{-20}$ J)			
$A_{232'3}$	$A_{2'312}$	$A_{231'2'}$	$A_{121'2'}$
7.1176	12.010	-1.1129	-1.9072

Table 2: Hamaker Constants for Head Disk Interface

(a)

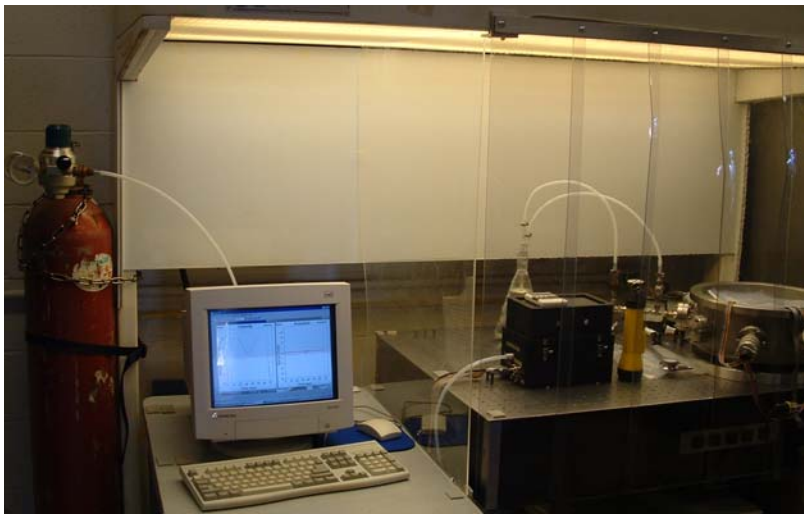

(b)

Figure 1: (a) Belljar apparatus; (b) Modified environmental chamber with N_2 gas cylinder.

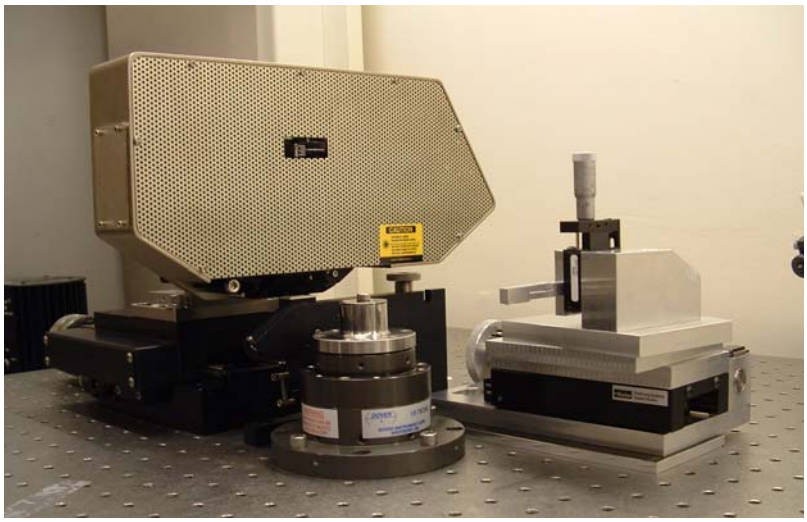

(a)

(b)

Figure 2: (a) Candela Optical Surface Analyzer (OSA); (b) Olympus Optical Microscope

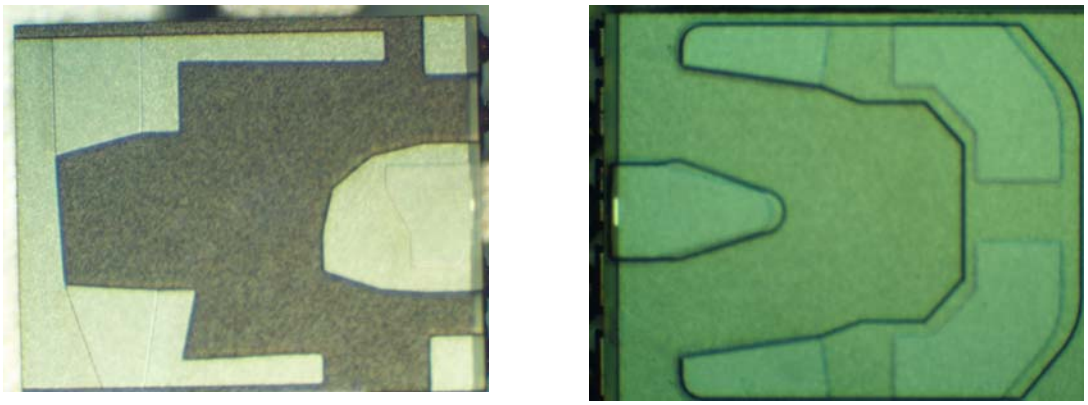

(a) (b)

Figure 3: (a) 18 nm (pico) slider; (b) 7 nm CML (pico) slider

(Note: The ABS of 5nm design is very similar to 7 nm design)

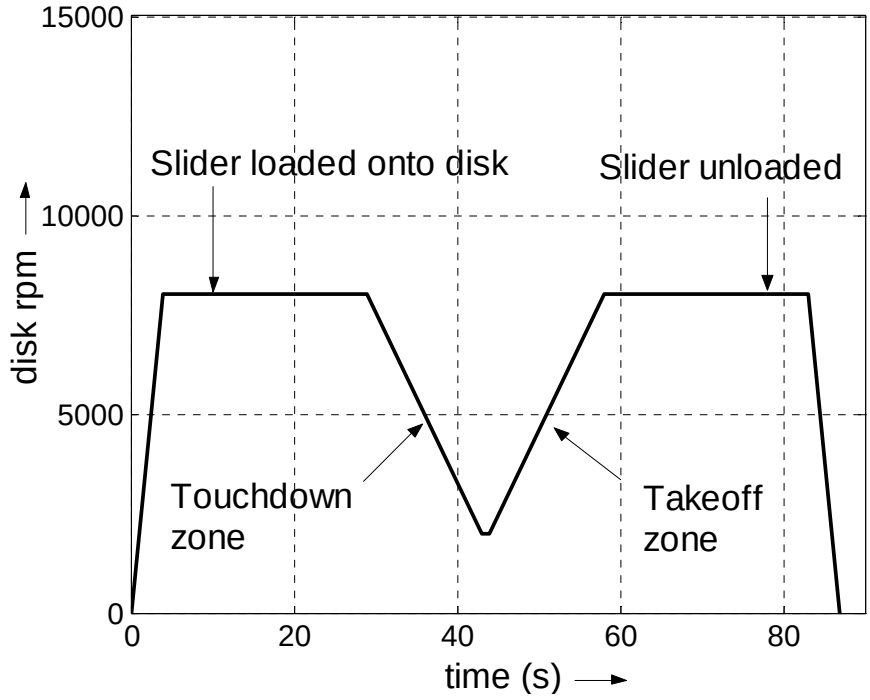

Figure 4: Velocity profile for Hysteresis tests

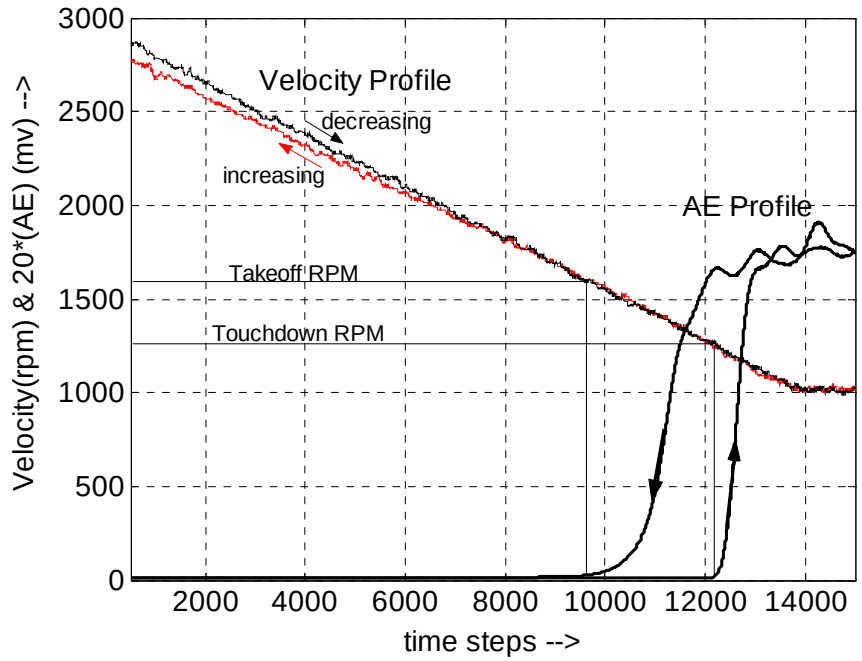

Figure 5: Hysteresis observed at zero humidity for 18nm slider.

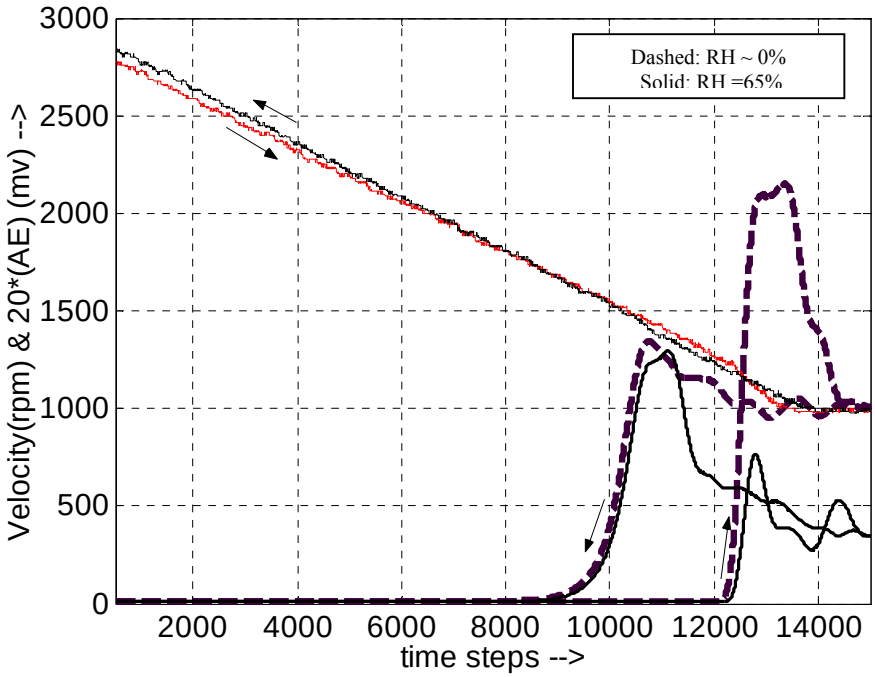

Figure 6: Dependence on ambient humidity

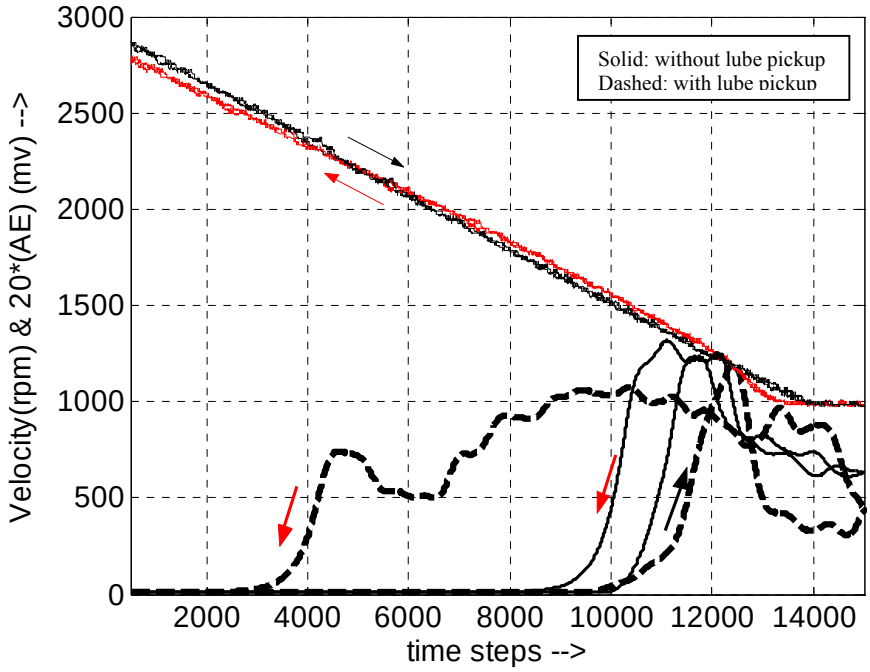

Figure 7: High hysteresis at high humidity: Lubricant pickup

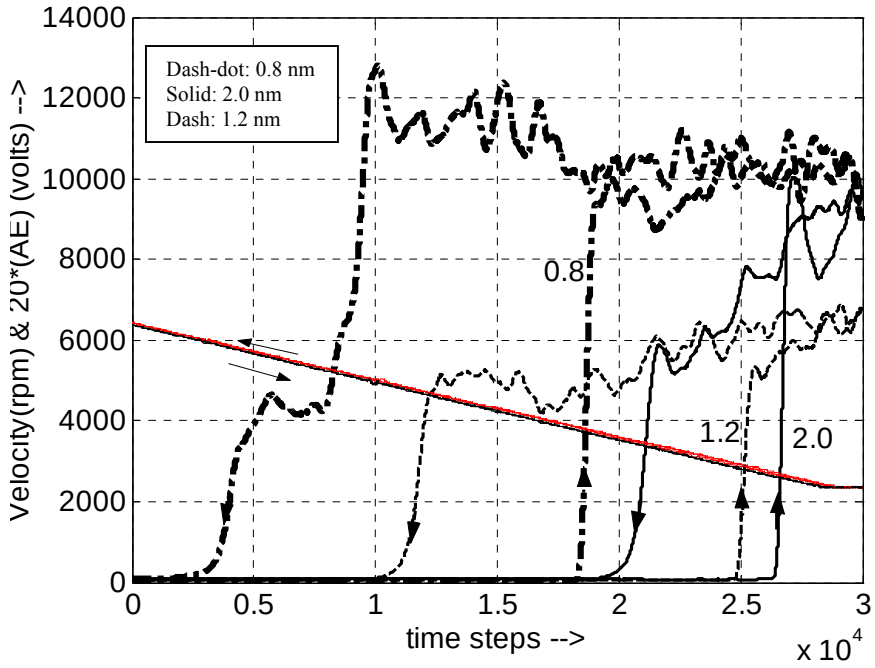

Figure 8: Hysteresis observed for various lubricant thicknesses (Red arm of velocity profile is spindown while the black arm corresponds to spin up.)

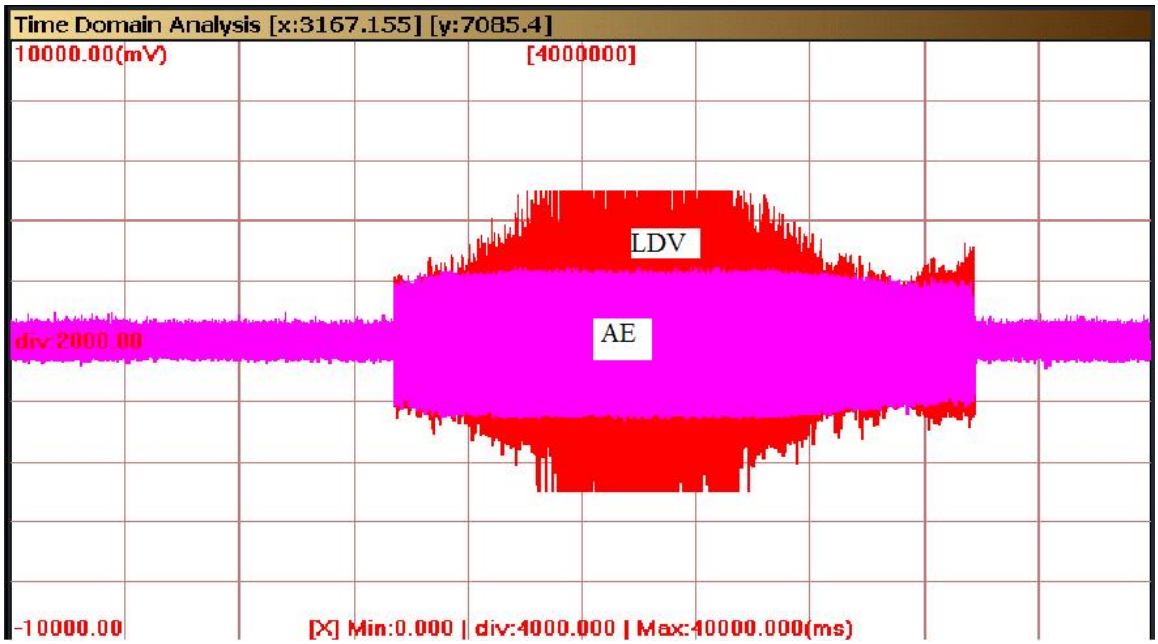

Figure 9: Comparison between AE and LDV signals for detection of contact

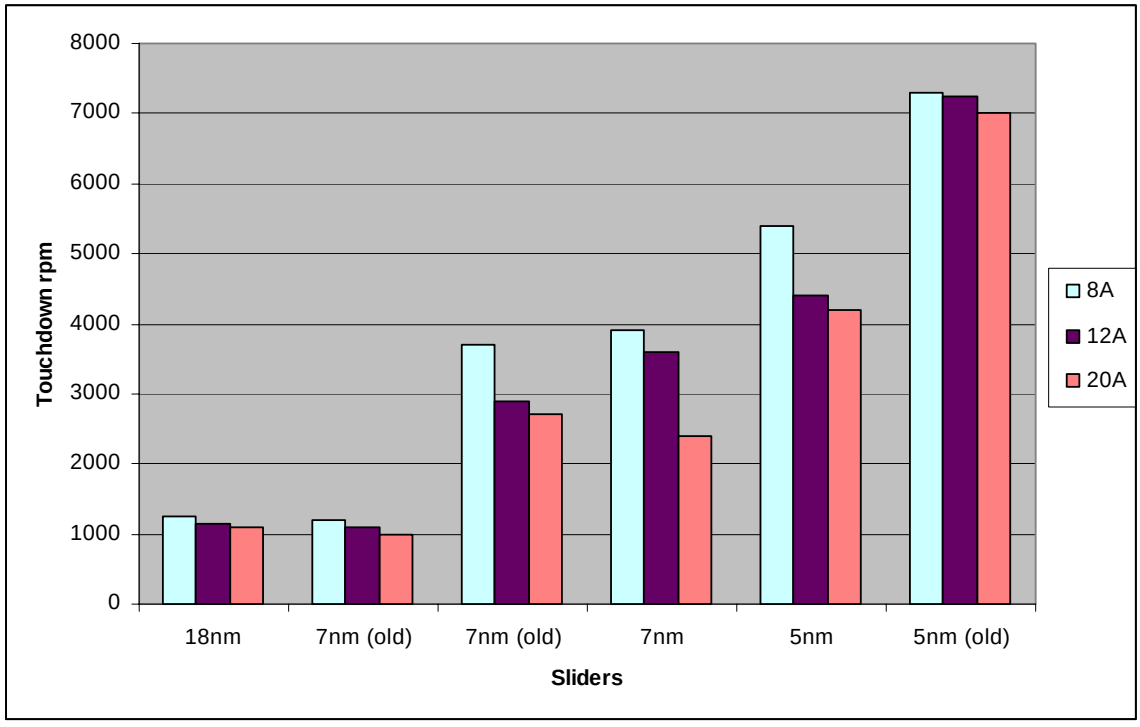

Figure 10: Variation of Touchdown rpm as a function of lubricant thickness for various slider designs (Experimental Results).

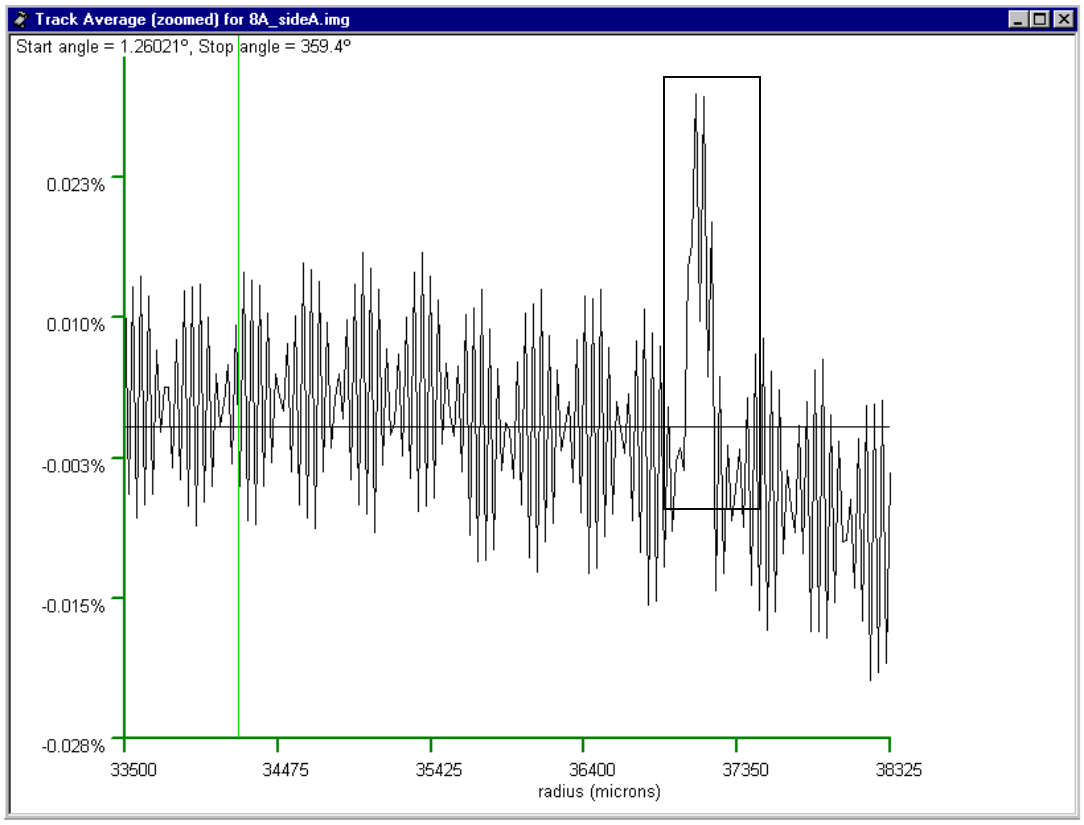
Track Average (zoomed) for 8A_sideA.img
Start angle = 1.26021°, Stop angle = 359.4°
0.023%
0.010%
-0.003%
-0.015%
-0.028%
33500
34475
35425
36400
37350
38325
radius (microns)

(a)

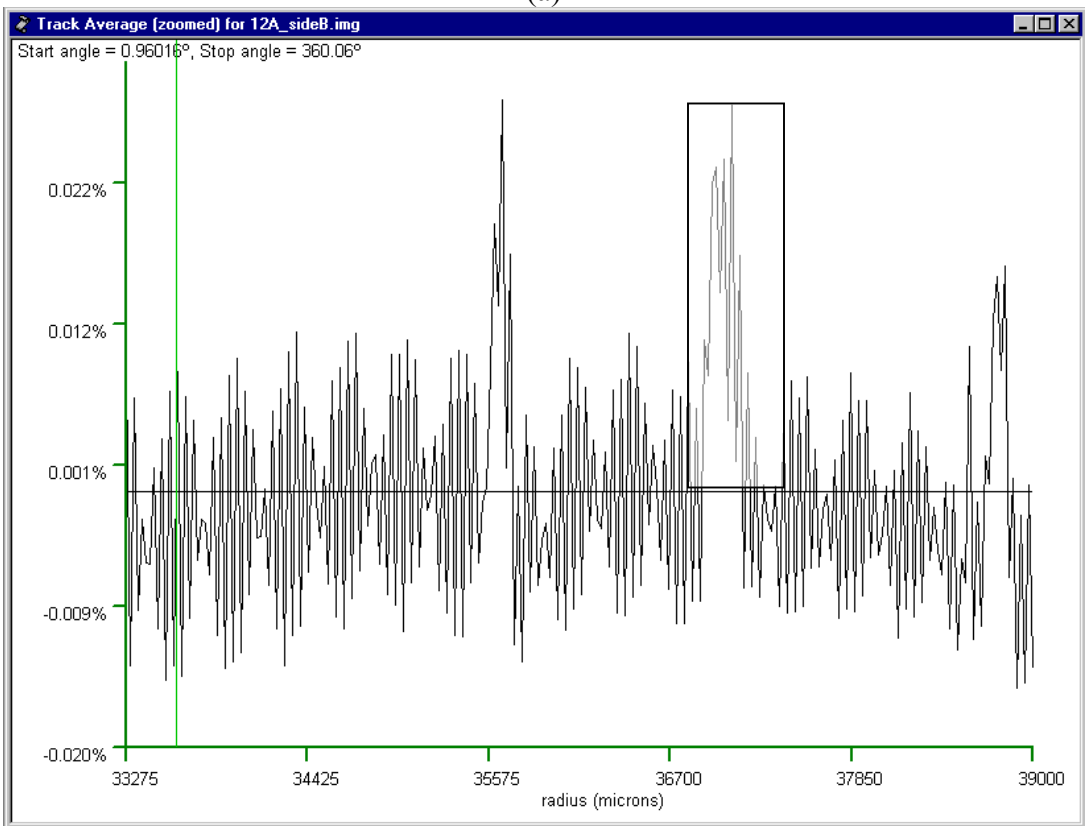
Track Average (zoomed) for 12A_sideB.img
Start angle = 0.96016°, Stop angle = 360.06°
0.022%
0.012%
0.001%
-0.009%
-0.020%
33275
34425
35575
36700
37850
39000
radius (microns)

(b)

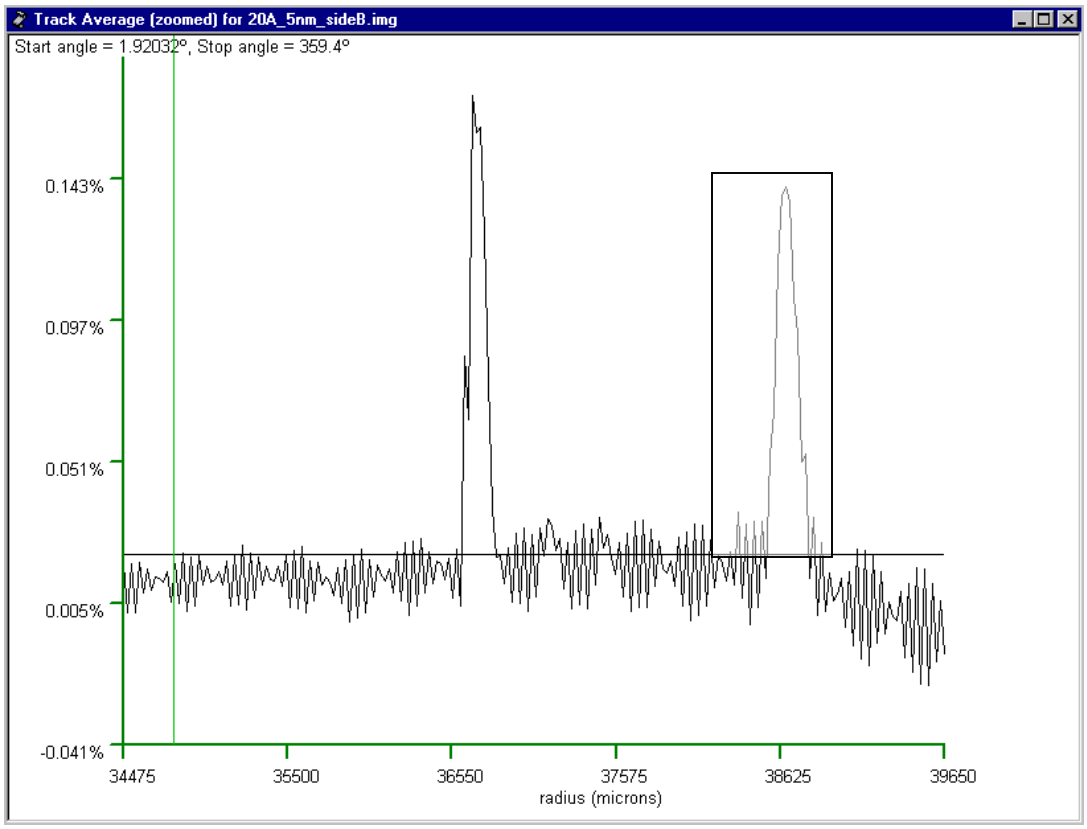

(c)

Figure 11: Track average of reflectivity against radius (microns) for different lubricant thickness after SDS test was conducted with 5nm slider:

(a) 8 Å, (b) 12 Å, (c) 20 Å; (Calibration factor ~ -0.0062 %/Å)

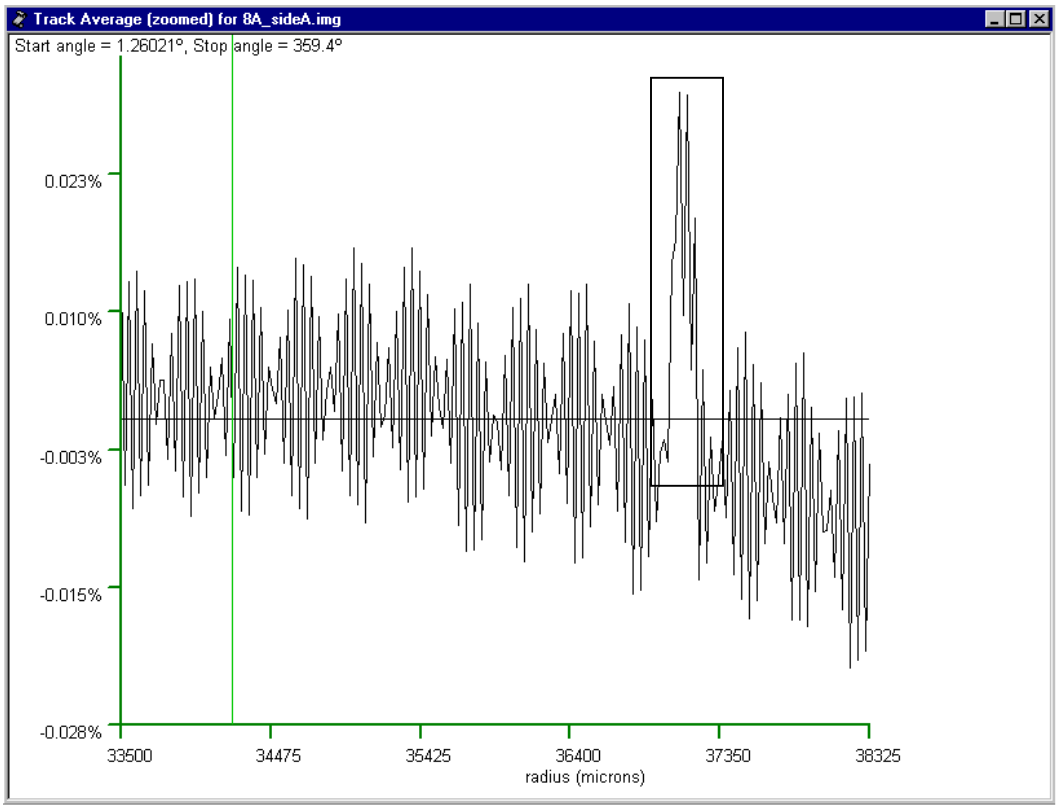
Track Average (zoomed) for 8A_sideA.img
Start angle = 1.26021°, Stop angle = 359.4°
0.023%
0.010%
-0.003%
-0.015%
-0.028%
33500
34475
35425
36400
37350
38325
radius (microns)

(a)

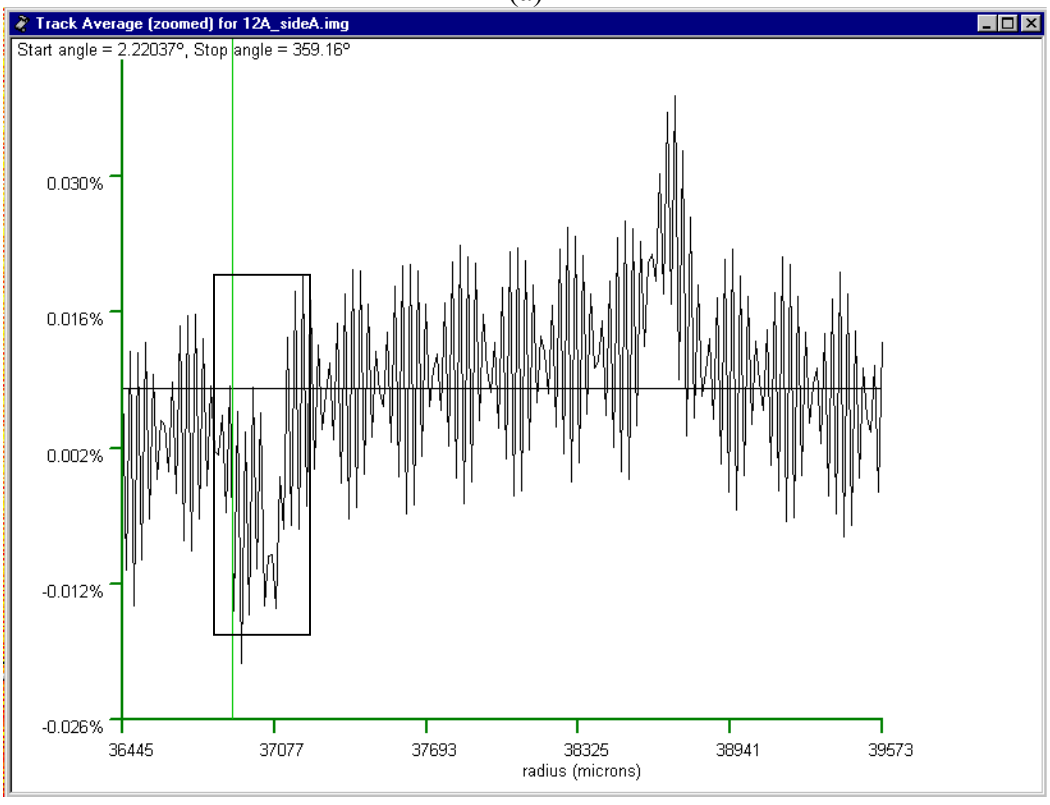
Track Average (zoomed) for 12A_sideA.img
Start angle = 2.22037°, Stop angle = 359.16°
0.030%
0.016%
0.002%
-0.012%
-0.026%
36445
37077
37693
38325
38941
39573
radius (microns)

(b)

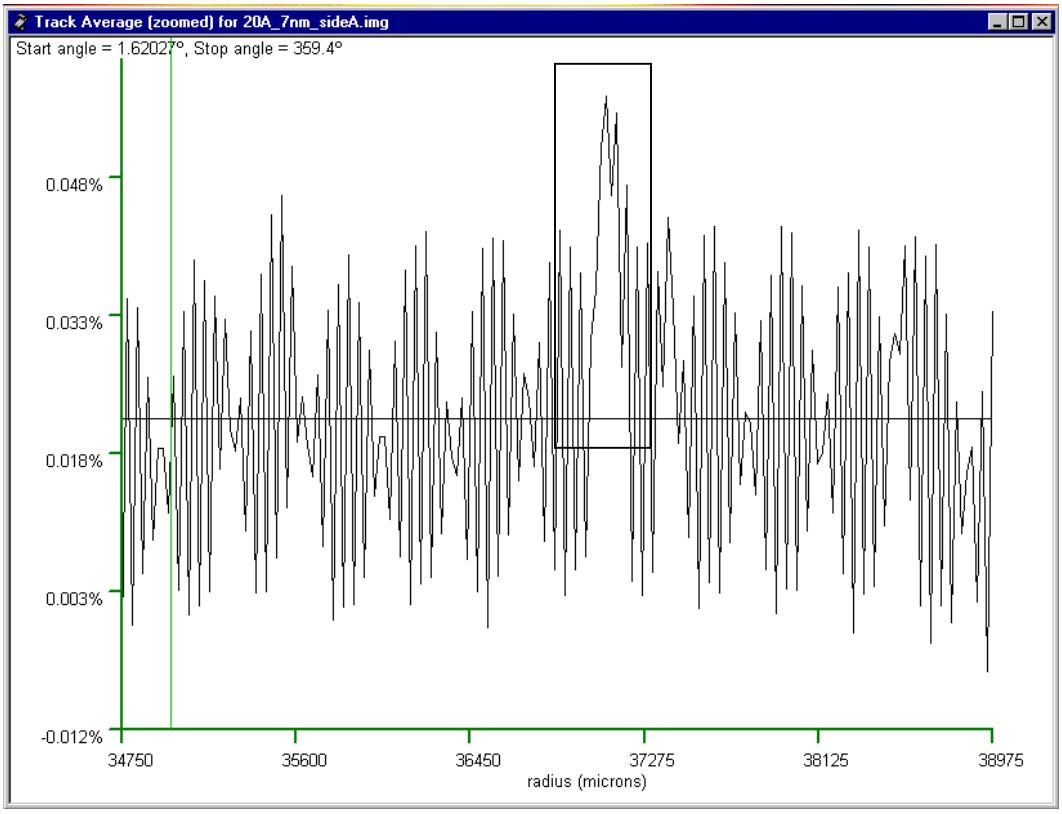

(c)

Figure 12: Track average of reflectivity against radius (microns) for different lubricant thickness after SDS test was conducted with 7nm slider:

(a) 8 Å, (b) 12 Å, (c) 20 Å; (Calibration factor ~ -0.0062 %/Å)

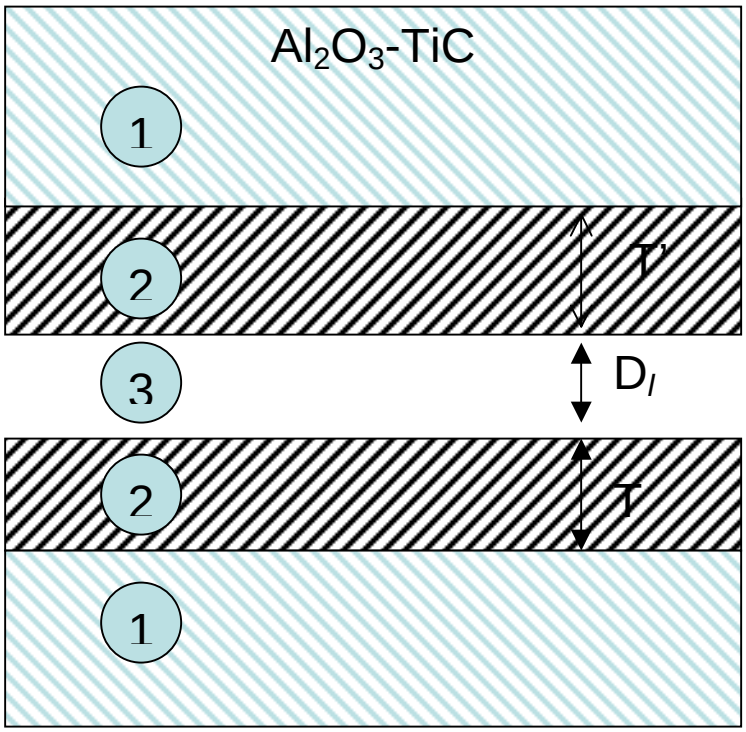

Figure 13: Multilayer model for modeling intermolecular forces

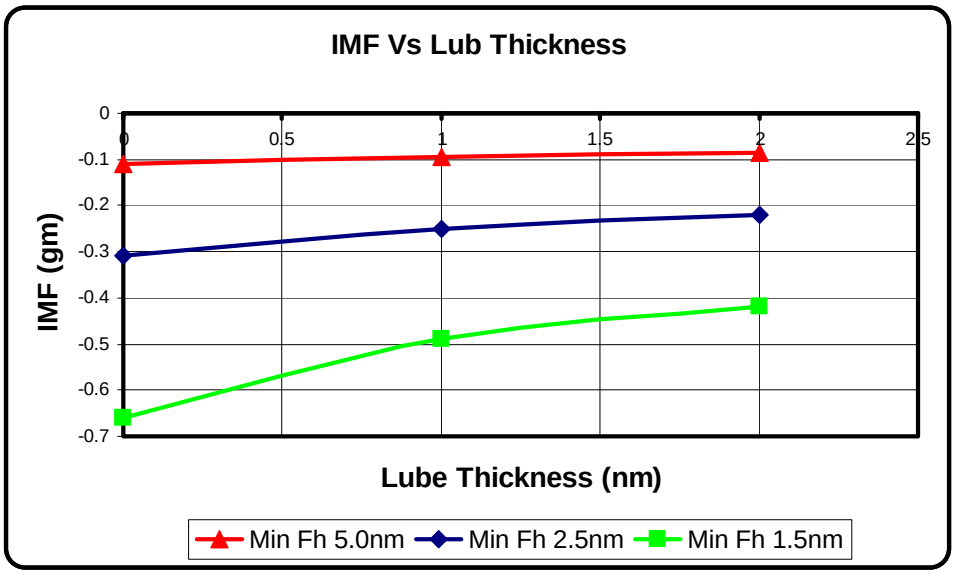

Figure 14: Variation of intermolecular forces as a function of lubricant thickness

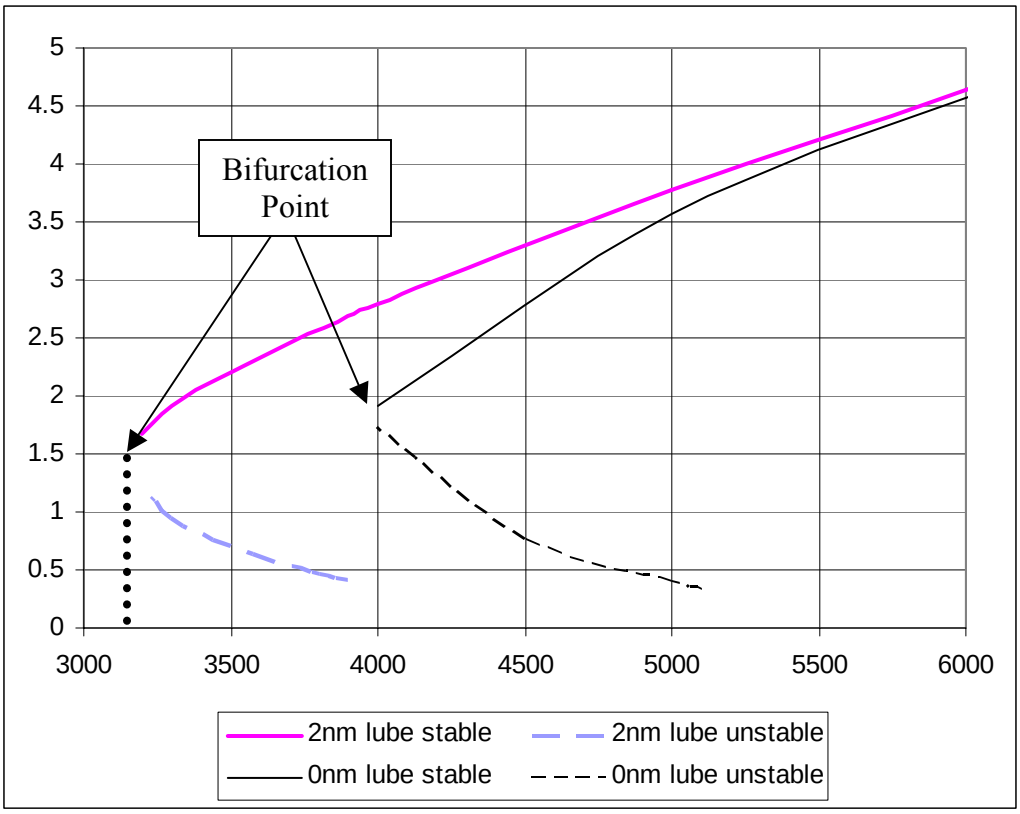

Figure 15: Fly height diagram (Simulations)

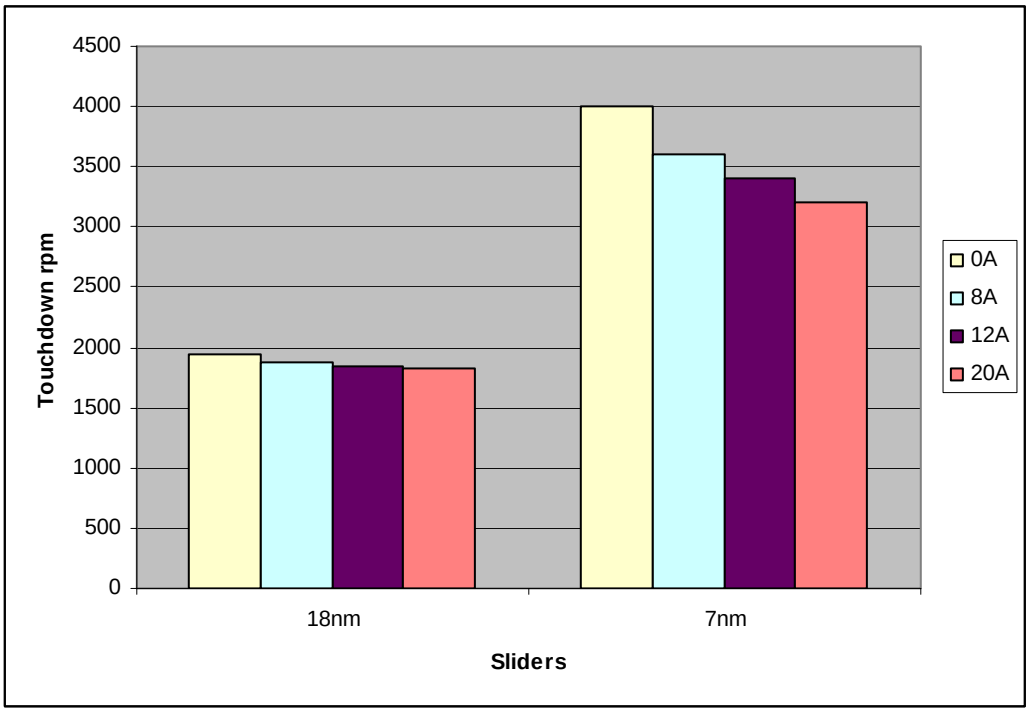

Figure 16: Variation of Touchdown rpm as a function of lubricant thickness for various slider designs (Simulation results)